6702ENG UAV Design

Project Report

Video Inspection RPAS Design

Title

Program Name:	Bachelor of Engineering (Honours)
Course Name:	6702ENG UAV Design
Report Title:	Video Inspection RPAS Design
Student:	Minh Man Ly s5160196
Supervisors:	Steven O'Keefe
	Daniel Peberdy
Start Date:	N/A
Due Date:	29th October 2021
Word Count:	

I hereby declare that, except where specifically indicated, the work submitted herein is my own original work.

Contents

Title **2**

1. Introduction **4**

2. Composition and Concept **5**

3. Propulsion System **7**

3.1 Motors and Propellers Analysis *7*

3.2 Flight Time Estimates *11*

4. Airframe Design **13**

4.1 Modelling *13*

4.2 Simulations *16*

4.2.1 Material Properties 16

4.2.2 Static Stress Analysis 17

6. Implementation **20**

6.1 Hardware *21*

6.2 Software *23*

7. Results **25**

8. Conclusions and Future Work **26**

References **27**

Appendix A: Link to Resources **28**

Appendix B: Mechanical Drawings **29**

1. Introduction

The versatility and diversity of unmanned aerial vehicles (UAVs) in shapes, sizes, types, and applications have been widely recognized for over a decade. The UAV quadrotor is a distinctive type of UAV that possesses the Vertical Take-Off and Landing (VTOL) ability that has a great advantage of maneuverability thanks to its inherent natural dynamics [1]. The design of UAV quadrotors has attracted extensive attention from drone hobbyists and engineers, namely Zimmerman [2] and Salmony [3].

Depending on specific applications, design considerations and specifications must be known in the design of the UAV quadcopter. Some of the quadcopter specifications include airframe configuration, required thrust, maximum takeoff weight (MTOW), power requirements, and payloads. Components chosen in the design are important in properly constructing the aircraft to match the specifications. Some of the common components found in a quadcopter include flight controller, motors, propellers, battery, and GNSS module. Each component has its specifications which make the design of a quadcopter unique. The design considerations are of great importance when it comes to building a functioning RPAS as they affect various aspects in multiple design phases. The quadcopter building process is a design loop that repeats itself during all optimization phases in which assumptions can be made and components are selected based on those assumptions [4].

This project aims to design and build a UAV quadcopter from off-the-shelve components that targets at video inspection application. Additionally, the project delves into the development process and design validation by means of simulation and analysis to satisfy safety requirements. Eventually, a demonstration of test flight is to be performed under the supervision of Griffith University's certified UAV professionals, Steven O'Keefe and Daniel Peberdy.

The video inspection mission objective is that the designed RPAS must be able to fly to a location and transmit video back to the pilot. The pilot must be able to adjust the pitch of the camera. The camera does not need to be gimbal mounted.

This UAV quadrotor design report contains the following:

- Discussion of the design process and validation of design and safety decisions made
- Discussion of the manufacturing methods chosen
- Photographic record of the manufacture
- Full shop drawings and electronics schematics
- Discussions on the safety analysis performed for test flights
- Test flight results and tuning procedures
- Conclusion discussing outcomes, recommendations, and future work

2. Composition and Concept

To be able to design a proper airframe and to select suitable components to satisfy UAV quadcopter performance requirements, it is necessary to have some understandings and estimations on the design. In addition, developing a model of the quadcopter will give an insight into factors that influence a quadcopter's behavior in terms of its stability and performance. This section gives a brief introduction to UAV quadrotors, basic components, estimation which becomes the basis for later design considerations.

An X-shaped quadcopter was to be used as the main configuration for the airframe with its benefits and 3D model detailed in section 4. A basic model of the configuration is shown in Fig. 1a) where all propellers are spinning towards the fuselage. In order for a drone to take off and hover, weight and drag must be overcome. In particular, the weight of a drone is the force acting on it due to gravity and drag is the force acting opposite to the relative motion of the drone to resist its movement through the air. The thrust generation from the rotation of propellers enables the drone to take-off and maintain airborne if that thrust is equal to or greater than the drone's total weight. For instance, if a drone weighs 777g, a total thrust of 7.6N, or 1.9N per propeller, (assuming gravity = 9.8m/s^2) is required for the drone to hover (Fig. 1b). It is important to note that the peak thrust produced by a propeller should be twice the quadcopter's weight to maintain good control stability. Thus, in the above example, to maintain a 2:1 thrust-to-weight ratio, the total thrust produced by all four propellers must be 15.2N. A greater thrust-to-weight ratio is recommended, especially in racing quadcopters. However, more thrust may lead to less overall system efficiency which consequently reduces flight time.

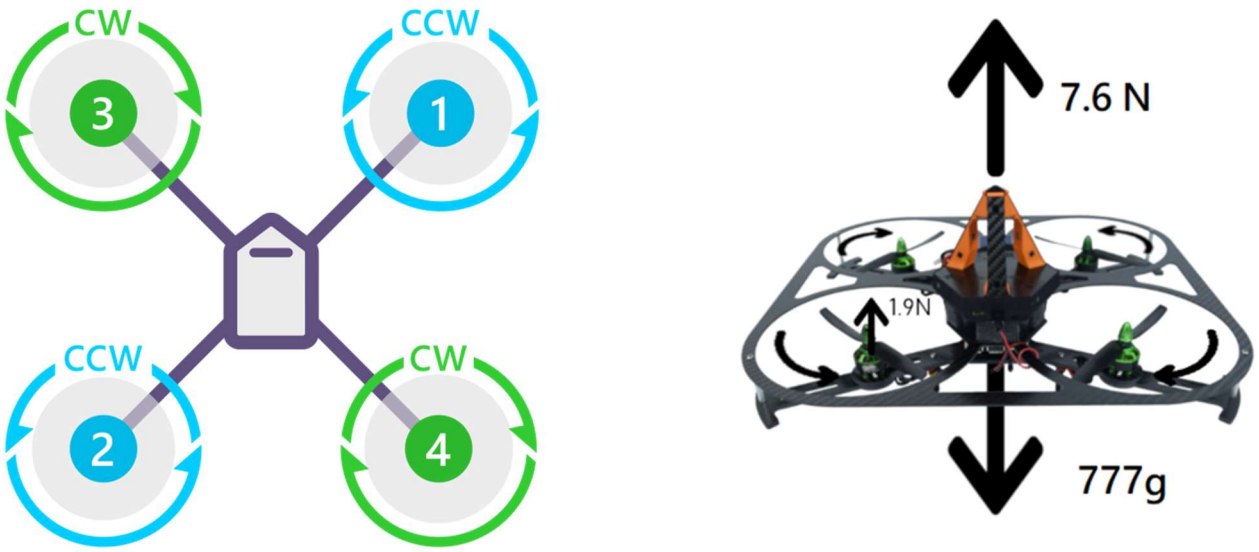

(a) Rotation direction of propellers

(b) Weight and thrust at hover

Figure 1: Basic operation of a quadcopter [5, 6].

Basic electronic components of the RPAS to be built in this project are listed in Table 1 with their masses. At the time of measuring the components and estimating total mass of the quadcopter, motors, propellers, and electronic speed controller (ESC) had not been decided yet.

Electronic component	Mass (g)	Description
Flight controller	39.28	Pixhawk 2.4.8 flight controller
Telemetry module	39.4	915MHz V5 radio telemetry
Power module	43.13	GM v1.0 Pixhawk power module
GPS module	28.56	M8N GPS module with compass
Carbon plates	16.55	Anti-vibration damping plate to mount the Pixhawk flight controller
Power button	1.6	
Buzzer	2.56	
Camera and antennas	23.78	FPV camera and TS5823 32CH 5.8HGz video transmitter
RC receiver	14.82	FlySky – iA6B 2.4GHz RC receiver
Servo	9.0	SG90 micro servo
Motors	160 (estimated)	N/A
Propellers	30 (estimated)	N/A
ESCs	30 (estimated)	N/A
Total	438.68	

Table 1: Estimated masses of projected components to be used in the final design.

Before the design process and proper experiments could be established, some assumptions were made on the desired UAV quadcopter. These assumptions depended on the project's requirements such as application, and payload. Furthermore, the assumptions were based on the intended material to be used in the main airframe as physical properties and characteristics of materials are all different, impacting the design considerations. Estimations for the quadrotor RPAS can be found in Table 2 below. It is important to note that these parameters were outlined at the beginning of the design phase which means that most of these parameters would change at the end of the design.

Parameter	Value/Material	Description
Airframe mass	0.7kg	Total weight of the RPAS with payloads excluding battery
Maximum Take-off Mass (MTOM)	1.9kg	Maximum permitted mass of RPAS before take-off including all payloads and battery
Airframe material	Polylactic Acid (PLA)	PLA filament for 3D printer
Desired peak thrust per propeller	1.2kg	Maximum thrust produced by one propeller within ESC current capability
Flight time	15 minutes	Endurance based on airframe weight, average power consumption, and battery
ESC current capability	30A	Current capability of ESCs
Battery capacity	5000mAh	
Battery mass	0.5kg	
Battery configuration	Lipo 4S	4 cells connected in series with 3.7V nominal voltage per cell
Battery C-rating	>= 25C	The measurement of current in which a battery is charged and discharged at

Table 2: Estimated quadrotor parameters for the final design.

3. Propulsion System

The design of UAV quadrotor propulsion system is an optimization loop that starts at initial assumptions on a desirable system [6]. Making assumptions and choosing a propulsions system based on those assumptions before the first version of the RPAS is realized is a challenging process as a single modification or a change in initial design ideas could cost the project time, effort, and budget. Thus, tests and simulations must be performed in each stage of the design, and changes are made in time with respect to outcomes.

The design loop (Fig. 2), proposed in [6], was employed in this project to aid the motor and propeller design phase. Indeed, the given method was very useful in enhancing flight time and performance of a quadcopter. Details on the motor, propeller, and battery selection to maximize a multirotor flight time and lift capacity can be found in [6, 7]

The goal of this section is to demonstrate the process of developing and evaluating a propulsion system consisting of propeller and motor for the quadrotor RPAS to optimize endurance and lift capacity. The decisions made in this section were partially based on the estimations discussed in the previous section.

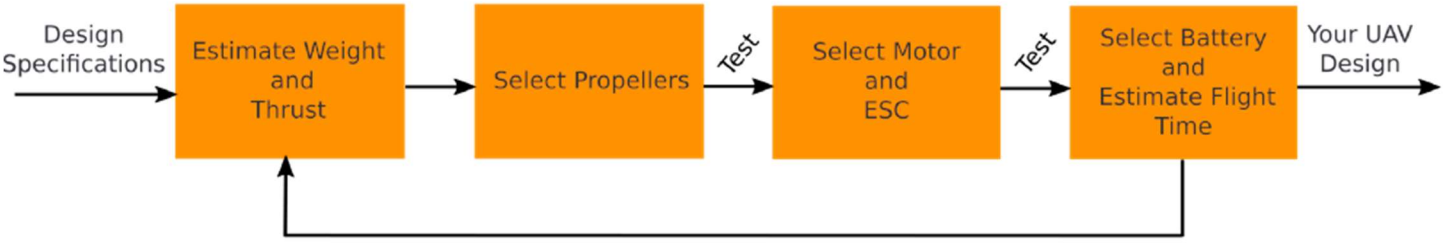

Figure 2: Propulsion system design loop for multirotor [6].

3.1 Motors and Propellers Analysis

Motor and propeller are fundamental components in every VTOL RPAS as they generate thrust to lift the aircraft and affect control stability. Motor type does not influence thrust generated by propellers since propellers with the same physical properties are equivalent in terms of thrust when paired with different brushless direct-current (BLDC) motors as long as the propellers are spinning at a specific rotational speed measured in rotations per minute (RPM). Yet, system efficiency is different among propeller and motor setups which ultimately has an effect on the endurance or flight time of an RPAS. Furthermore, motors affect maneuverability in multirotor RPAS due to one motor being able to accelerate the propeller faster than another.

The overall performance of a quadcopter depends on a well-balanced combination of motor and propeller that satisfies design specifications. The overall system efficiency can be calculated using Eq. (1). Changing the motor, propeller, or even the ESC contributes to varying the system efficiency

$$System\ efficiency\left(\frac{kgf}{W}\right) = Propeller\ efficiency\left(\frac{kgf}{W}\right) \times Motor\ efficiency \quad (1)$$

The propeller efficiency is defined as propeller thrust divided by mechanical power applied while the motor efficiency derives from the electrical power being converted into mechanical power. During the power conversion of the motor,

heat losses are inevitable due to the imperfection of BLDC motor caused by friction, iron losses, and copper losses. Eq. (2) and Eq. (3) give the formulas to calculate propeller and motor efficiency, respectively.

$$Propeller\ efficiency\ \left(\frac{kgf}{W}\right) = \frac{Thrust\ (kgf)}{Mechanical\ power\ (W)} \tag{2}$$

$$Motor\ efficiency = \frac{Mechanical\ power\ (W)}{Electrical\ power\ (W)} \tag{3}$$

Determining the efficiencies allows flight time estimation for an RPAS built with a given motor-propeller setup to be done. The endurance of the RPAS, which can be estimated using Eq. (4) is dependent on weight, battery specifications, and system efficiency.

$$Flight\ time\ (h) = \frac{Battery\ energy\ (Wh)}{Average\ power\ consumption\ (W)} \tag{4}$$

Details on specifications and the effect of propeller and motor parameters such as rotational speed, torque, back electromotive force (EMF), velocity constant, and torque constant on an RPAS will not be discussed in this report.

Data on efficiencies, thrust, and power consumption were measured and calculated using a brushless motor and propeller test stand that was the RCbenchmark dynamometer. Seven motor and propeller combinations were tested which yielded the results shown in Fig. 3. 8-inch, 9-inch, and 10-inch propellers were tested since propellers with small dimensions would provide insufficient thrust required for the estimated quadcopter's weight, while larger propellers demand high current which increases the size, weight, and capability of electronic speed controllers (ESCs). A larger propeller may provide excess thrust, yet it put a constraint on airframe design and material selection which will be discussed in section 3. Propellers that have 5- and 6-inch diameters were tested in previous work done by the author [8], indicating insufficient thrust for the estimated 1.2kg quadcopter (Table 1). The procedure to collect motor and propeller data is outlined in [8].

Fig. 3 plots the system efficiency with respect to thrust for each tested propeller-motor combination. It can be observed from the figure that the 1045 propeller paired with 2810/1180Kv motor produced a significant amount of thrust, around 1.6kgf, at full throttle. This combination also maintained excellent system efficiency above 0.4kgf thrust, ranked second only behind 9450 - 2312A/800Kv configuration. The combination of 9450 propeller and 2312A/800Kv motor was not capable of generating an excessive amount of thrust, with only 0.9kgf peak thrust, at max RPM produced by 800Kv motor. This could be a potential problem in the event that the total mass of the quadcopter exceeded the estimated value of 1.2kg. Yet, this combination excelled in terms of system efficiency which was useful in maximizing the endurance of the quadcopter. 1045 – 2812/1180Kv and 9450 – 2312A/800Kv combinations were the two biggest candidates for the required RPAS in this project. Table 2 summarizes crucial information relating to seven tested propeller and motor systems for evaluation. Parameters shown in Table 3 were calculated using Eq. (1), (2), and (3). A thrust-to-weight ratio of 3:1 was preferred to preserve sufficient control stability.

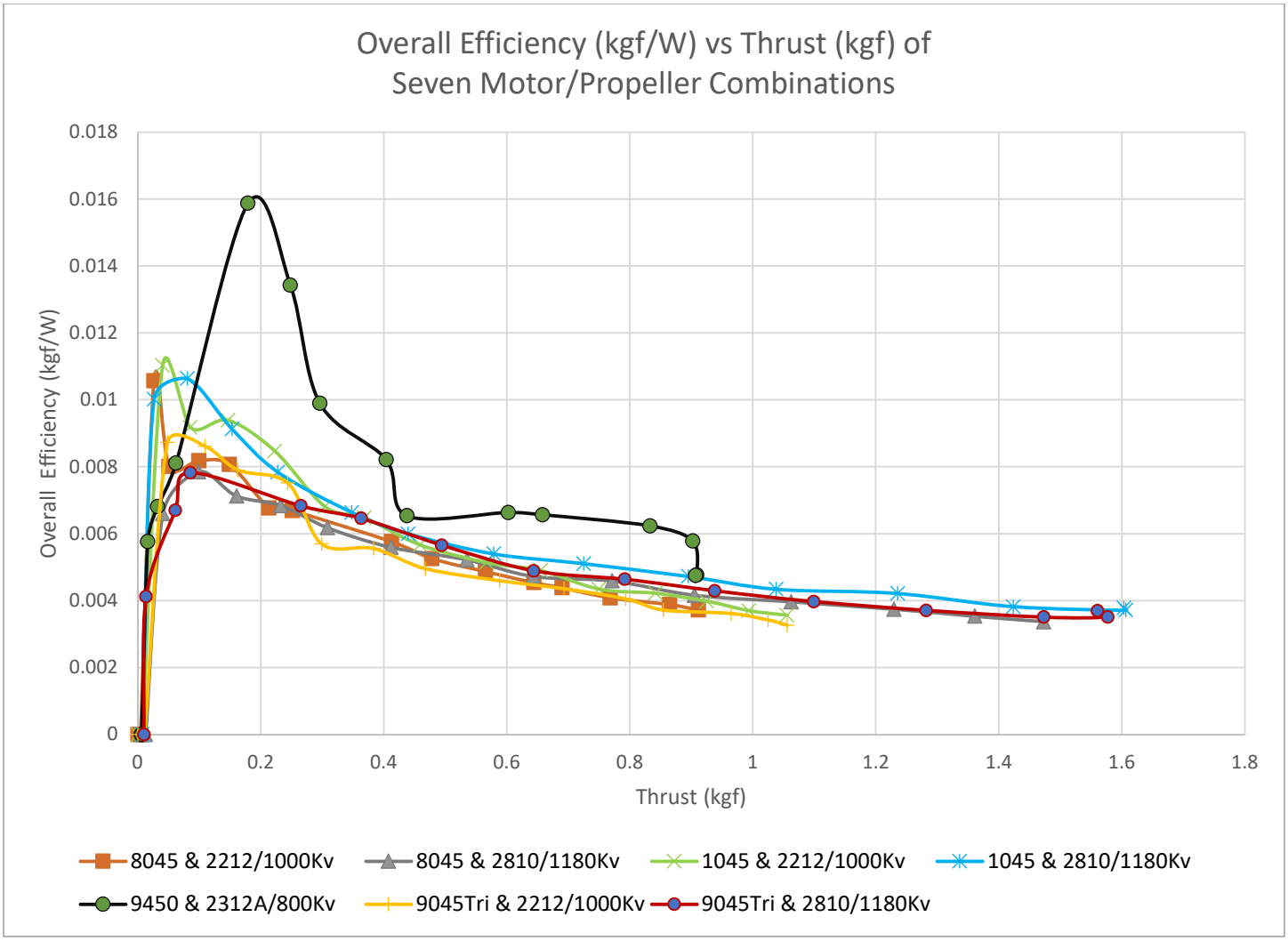

Figure 3: Overall system efficiency of tested motor-propeller combinations.

Propeller	Motor	Hover			Desired control authority (3:1 ratio)		
		Thrust (kgf)	System Efficiency (kgf/W)	Electrical Power (W)	Thrust (kgf)	System Efficiency (kgf/W)	Power Consumption (W)
8045	2212/1000Kv	0.307	5.913E-3	51.923	0.905	3.692E-3	245.163
8045	2810/1180Kv	0.303	6.801E-3	44.566	0.905	4.162E-3	217.447
9450	2312A/800Kv	0.302	9.405E-3	32.059	0.905	4.808E-3	188.359
9045Triblade	2212/1000Kv	0.305	5.594E-3	54.640	0.903	3.661E-3	246.838
9045Tribalde	2810/1180Kv	0.300	6.755E-3	44.451	0.903	4.369E-3	206.794
1045	2212/1000Kv	0.304	6.810E-3	44.697	0.907	3.988E-3	277.388
1045	2810/1180Kv	0.300	7.437E-3	40.338	0.902	4.604E-3	196.109

Table 3: Key parameters at hover and 3:1 control ratio of tested motor-propeller combinations.

During this stage, decisions were made on a propulsion system for the quadcopter. Priority on system efficiency was preferred to extend the endurance of the RPAS, even though this might risk the 3:1 thrust-to-weight ratio if the quadcopter's mass increased in later stages. Yet, proper airframe estimations and simulations had shown that the total mass of the RPAS would not be greater than 1.8kg, at which mass the thrust-to-weight ratio was downed to 2:1 (Airframe design and simulations on the RPAS will be discussed in section 4 and 5, respectively). Specifically, at minimum control authority of the 2:1 ratio, each propeller must produce 0.45kgf hovering thrust and 0.90kgf peak thrust in which the 9450 propeller and the 2312A/800Kv motor had satisfied. Regarding torque, the combination was capable of producing 0.115N.m torque at peak thrust. In addition, the 9450 propellers and the 2312A/800Kv motors were available resources provided by project supervisors which reduced the budget and shipping time to purchase new components.

Practically, in the worst-case scenario where the propeller cannot produce enough thrust to maintain the 2:1 ratio, the design loop mentioned at the beginning of this section (Fig. design loop) repeats to select a better propulsion system. In the case of our project, if the 9450 – 2312A/800Kv combination showed its lack of thrust at the end of all the design stages, the 1045 – 2810/1180Kv system could be an ideal alternative even though the airframe may need modifications. The 9450 propeller and the 2312A/800Kv motor can be seen in Fig. 4.

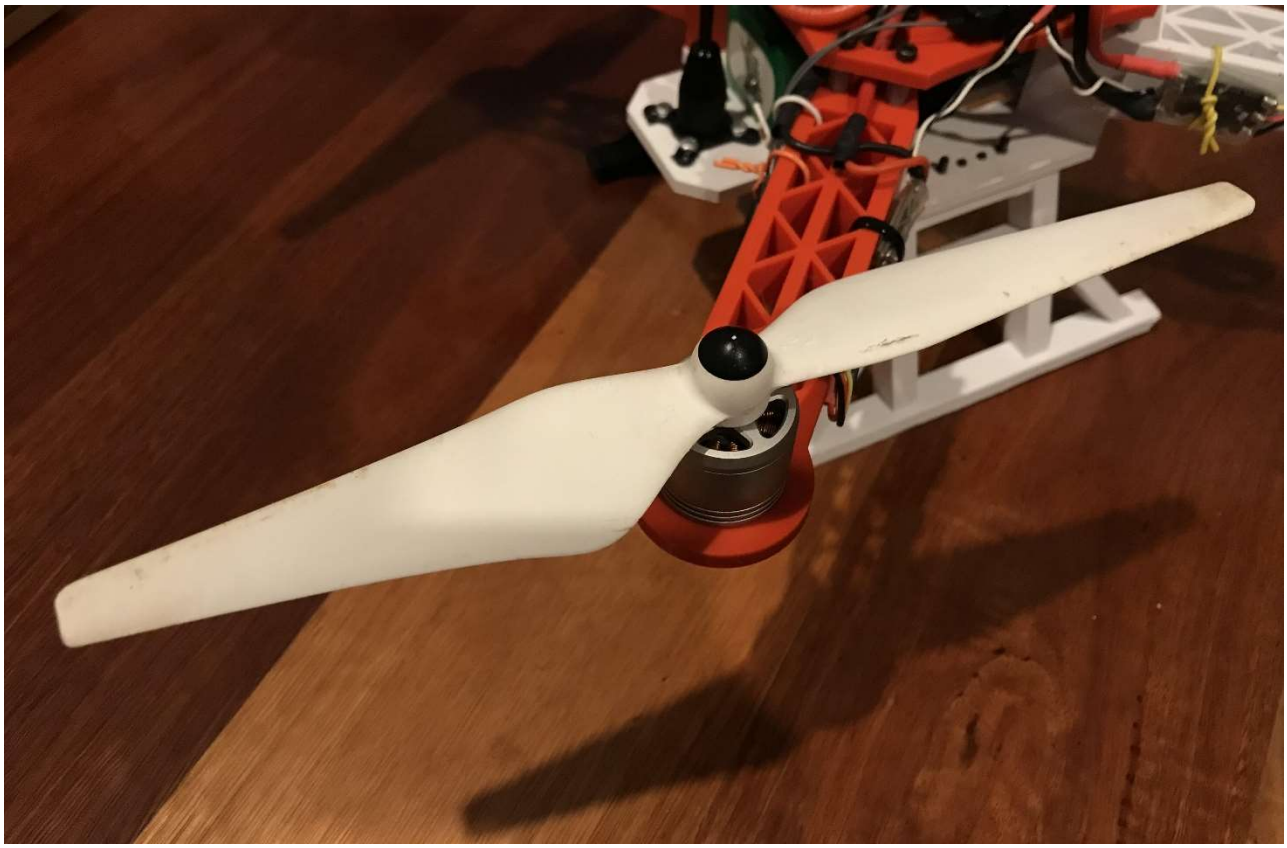

Figure 4: 9450 propeller paired with 2312A/800Kv motor positioned on one arm of the final design.

3.2 Flight Time Estimates

After the most efficient propeller and motor combination were selected, ESC was chosen to operate the 2312A/800Kv motor. However, because the ESC test was out of scope in this project, a brief description of ESC to match with propeller and motor was given in this sub-section rather than a detailed process. From Table 2, the electrical power consumption of the 9450 – 2810/800Kv was 32.059W and 188.359W at 0.3kgf and 0.9kgf thrust, respectively. The motor was driven by a 16.4V out of 30A power supply bench that is equivalent to a fully charged 4S battery. With the help of Eq. (5), the peak current to produce 0.9kgf of thrust per propeller was approximately 12A. For a hovering flight, the current was only 2A per propeller. This meant that a normal ESC having a current rating of 20A to 30A would deliver the motor's peak current. The ESC used in the RPAS of the project had a current rating of 20A with a small dimension that was useful in reducing the total weight of the quadcopter.

Apart from ESC, the current consumption of the motor was a concern in the battery selection. Battery selection was the last step before flight time estimates could be done. With each motor requiring 12A to operate to drive the propeller at peak thrust, the selected battery must be capable of delivering 60A at peak discharge. For a constant discharge rate, 8A to 12A was required. Several battery candidates are listed in Table 4 with their specifications and estimated flight time when they are used in a 0.7kg quadcopter airframe with payload (excluding battery weight). A spreadsheet, provided by RCbenchmark in [8], was used as a tool to aid in flight time estimation. However, manual flight time calculation can be done with Eq. (5). It is important to note that the actual flight time might be 1 or 2 minutes lower than the estimated values due to the safety discharge limit and battery voltage being lower at high load.

From Table 4, Multistar 4000mAh, Turnigy 8000mAh, and NXE Power 5400mAh batteries stood out in terms of energy density and estimated flight time. The Turnigy battery had the highest estimated flight time with more than 25 minutes while the Multistar ranked second with around 23 minutes flight time. However, the Multistar battery was impressively light-weight which was important in reducing the total weight of the RPAS. In addition, a light-weight battery had an advantage in later design phases when the actual mass of the entire aircraft was more than the estimated mass of 1.2kg. The energy density of the Multistar battery was significantly higher than all other candidates. Yet, this battery was rated at 10C only which meant that it had a constant discharge rate of 40A. In the specification of the battery, it was capable of discharging at 20C, or 80A. Therefore, this seemed to be a suitable battery to be used for the project. The RPAS required for the project did not need a high discharge rate as indicated by the power consumption of the 2312A/800Kv motors. If the 1045 – 2810/1180Kv propeller and motor were used instead, the C-rating on the Multistar battery would be a great concern and a different battery with a higher C-rating must be chosen. For the application highlighted in this project, the Multistar 4000mAh 4S 10C Lipo battery was a perfect power source whose figure can be seen in Fig. 5.

Battery	Battery energy (Wh)	Battery weight (g)	Energy density (Wh/g)	Estimated RPAS weight including battery (g)	Estimated hover flight time (minutes)
Multistar 4000mAh 4S 10C Lipo [9]	59.2	320	0.19	1020	23.43
Ovonic 1300mAh 4S 100C Lipo [10]	19.24	160	0.12025	860	16.78
Ovonic 1800mAh 4S 100C Lipo [11]	26.64	218	0.12220	918	17.29
Turnigy 8000mAh 4S 12C Lipo [12]	118.4	752	0.15745	1452	25.78
Zop 5000mAh 4S 50C Lipo [13]	74	609	0.12151	1309	19.65
NXE Power 5400mAh 4S 60C Lipo [14]	79.92	554	0.14426	1254	22.02

Table 4: Estimated hover flight time of the 9450 – 2312A/800Kv propulsion system.

Figure 5: Multistar 4000mAh 4S 10C battery to be used in the final design [9].

4. Airframe Design

This section describes the airframe designed in 3D modelling software and validation of design via simulations. Simulations gave some understandings of how the airframe would behave under stress and load which was essential in ensuring safe RPAS operation.

4.1 Modelling

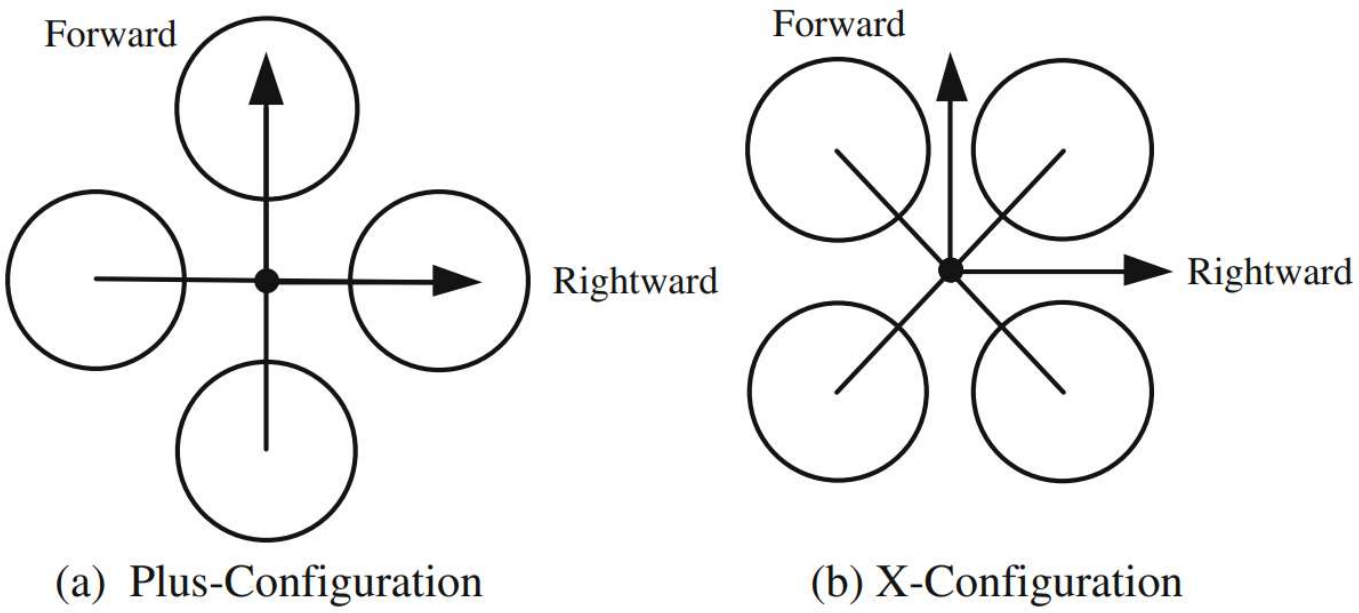

Figure 6: Cross configuration of a UAV quadrotor [15].

A cross configuration was used for the quadcopter. Particularly, the X-quadcopter has four propellers symmetrically distributed at the end of four arms in an X-shaped airframe as shown in Fig. 6. The X-shaped quadcopter has better maneuverability and less occlusion of the forward field of view compared to the quadcopter with plus-configuration [15]. The size of a UAV quadrotor, or a multirotor in general, is related to the radius of the propellers to be used in that UAV. The relationship between propeller radius and airframe radius is given by Quan in [15]. Let θ be the angle between two arms in a multirotor, then for an X-shaped quadcopter, θ = 90° (Fig. 7b). If the number of arms in a multirotor is n, the angle θ can be calculated to be

$$\theta = \frac{360°}{n}$$

Then, the relationship between the maximum radius of a propeller r_{max} and the airframe radius R is

$$R = \frac{r_{max}}{\sin\frac{\theta}{2}} = \frac{r_{max}}{\sin\frac{360°}{n}}$$

In order to prevent aerodynamic interference caused by propeller flow fields and cyclic fluctuation as indicated in [15], the following rule can be applied to airframe design

$$r_{max} = 1.05r_p \sim 1.20r_p$$

Therefore, the final equation to calculate suitable radius R for the quadcopter airframe can be defined

$$R = \frac{\beta r_p}{\sin\frac{360°}{n}} \tag{5}$$

where r_p is the propeller radius used in the quadcopter and β is the scale factor that ranges from 1.05 to 1.20.

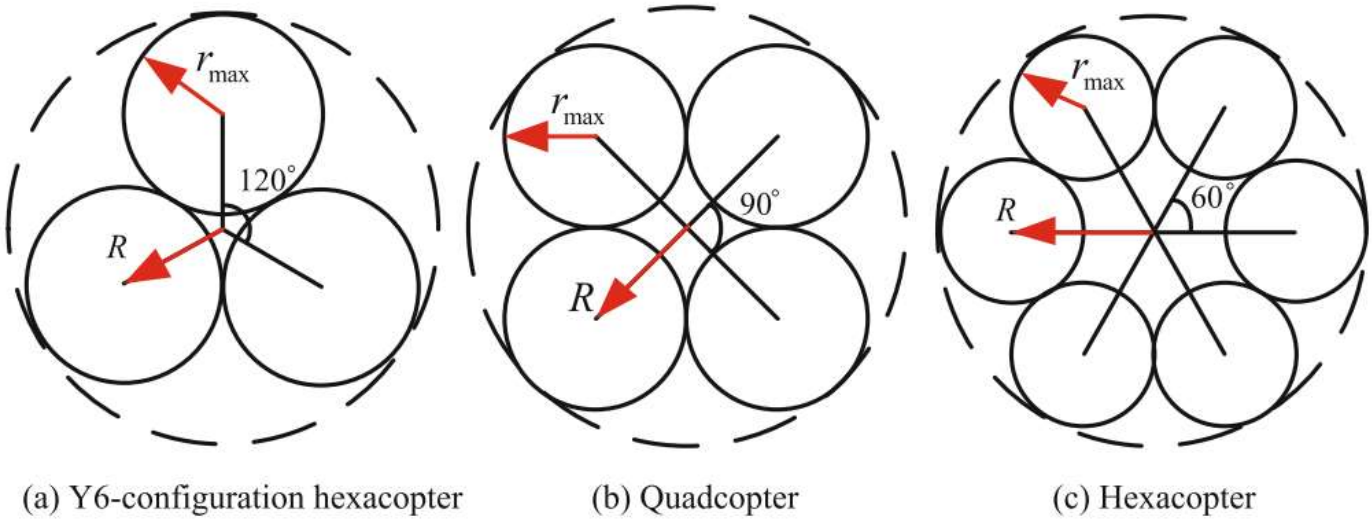

Figure 7: Multicopters with different configurations and their geometry parameters [15].

From section 2, the chosen propeller had a diameter of 9.4 inches, or 238.76mm. Thus, the 9450 propeller's radius r_p is 119.38. Giving the parameters: β = 1.15, r_p = 119.38, and n = 4, the airframe radius R was approximately equal to 195mm which was sketched in the model shown in Fig. 8. If the 1045 propellers were used rather than the 9450 propeller, the airframe radius R = 195mm would still satisfy the design with the new β parameter being 1.10.

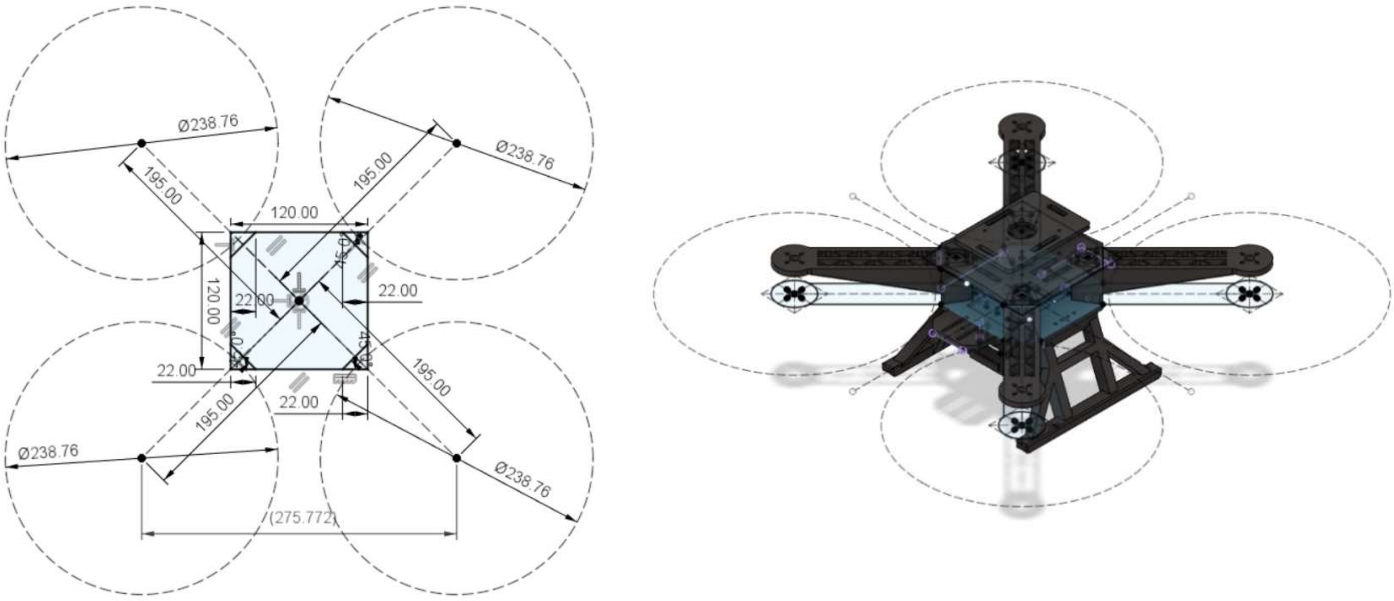

(a) Sketch dimension fitting 9450 propeller (b) 3D model based on propeller dimension

Figure 8: First sketch and model of the final design.

Due to the project requirement for the video inspection RPAS, a camera with adjustable pitch must be mounted to the quadcopter. In order to maintain stability, it is crucial that the center of gravity (CoG) of the quadcopter, or multirotor in general, is placed on the central axis, otherwise, the extra moment will be caused [15]. The effect of the position of CoG is discussed in detail in [15]. The CoG was affected by the position of the camera and payload on the RPAS. For higher stability, a low CoG configuration was chosen which meant that the camera was mounted underneath the RPAS. The camera mounted this way required the RPAS to be equipped with landing gear to protect the device during take-off and landing. A retractable landing gear was out of scope in this project; thus, simple landing gear was modelled. In addition, low CoG configuration with the camera mounted under the RPAS was more common and easier to be implemented.

Autodesk Fusion 360 software was used to 3D model the RPAS airframe. Polylactic Acid, commonly known as PLA, was used as the airframe material. The properties of PLA will be discussed in the next section. This material eased the manufacturing process as it is one of the most common materials used in 3D printing. Hence, the airframe was modelled so that each component in the airframe such as fuselage, arms, and landing gear was to be produced by the Prusa i3 MK3 3D printer. Using PLA filament also reduced the production cost to manufacture the airframe, and, in the event of broken airframe, a new airframe could be printed again easily. However, the PLA filament has some properties that require thorough consideration in the design of airframe. Fig. 9 and Fig. 10 show the completed modelled airframe for the video inspection RPAS.

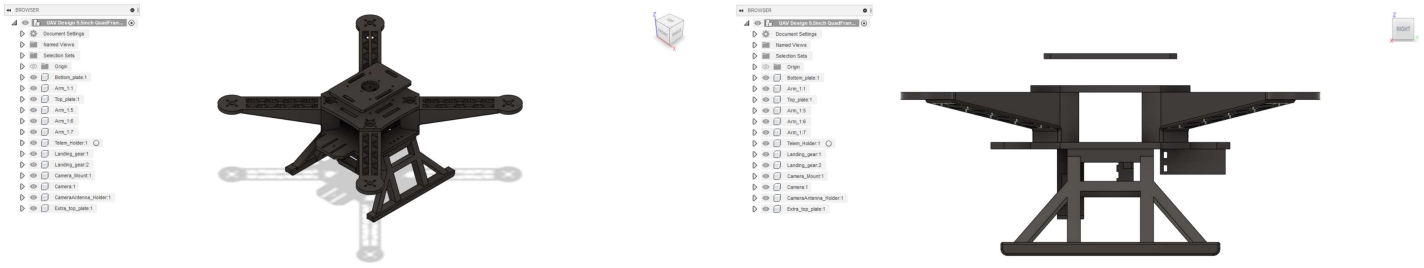

(a) Home view (b) Side view

(c) Front view (d) Top view

Figure 9: Different views of the modelled airframe.

Figure 10: Simulated center of mass (CoM) of the final airframe.

4.2 Simulations

Prior to airframe evaluation, material properties were thoroughly defined so that Autodesk Fusion 360 could properly perform simulation. Static stress to study thrust and torque induced on the airframe was done with results showing maximum safety factor, meaning the design was valid to be used in the project. Natural frequency and drop test were two other simulations that could be done to evaluate the design. However, these two simulations were never carried out due to the complexity in simulating a drop test and natural frequency serving no significant purpose in the design.

4.2.1 Material Properties

Because 3D printing was chosen as the manufacturing method for the airframe, Polylactic Acid (PLA) was the go-to material for the structure of the RPAS. PLA has several merits such as ease-of-use, low-cost, and dimensional accuracy [16]. Furthermore, the material is one of the most environmental-friendly filaments, being renewable and biodegradable, as it is derived from crops such as sugarcane and corn [16]. When it comes to physical and mechanical properties, PLA is not a bad option to be used in UAV multirotor as it has good stiffness and strength. The main properties of PLA used in the simulation are shown below. These properties were adapted from [16, 17].

- Density: 1.250g/cm^3
- Young's modulus: 3.500GPa
- Poisson's ratio: 0.36
- Yield strength: 70.000MPa
- Ultimate tensile strength: 73.000MPa

- Thermal conductivity: 1.260E-01W/(m.K)
- Specific heat: 1.280J/(g.°C)

However, PLA is not a perfect material since it possesses several disadvantages. The material has low heat resistance which means it is not suitable for prolonged outdoor activities. Extended time under sunlight exposure will result in the reduction of endurance for PLA material. In addition, although PLA is characterized by excellent tensile strength and other basic properties, it is rigid and brittle at room temperature [17]. Therefore, as indicated in [17], the inherent brittleness of PLA is a major bottleneck for its large-scale commercial uses. Because of these disadvantages, PLA must be used with precautions in the quadrotor airframe. For this project, to ease the manufacturing process and lower the cost, PLA is appropriate as a quick prototype for the RPAS with moderate thrust generation and minimal sunlight exposure.

With PLA being the main material for simulations, the mass of the quadcopter could be realized based on physical properties of the material. The estimated masses of each component in the airframe are shown in Table 5. The estimated mass of the modelled airframe was approximately 660g, yet this mass did not consider infill type and infill percentage for 3D printing. Assuming 40% infill percentage, the total mass would be brought down to 264g. This would leave 436g for all payloads, excluding battery, to make up 700g estimated quadcopter's mass proposed in section 1. Yet, 264g for airframe and 436g for payloads were not a safe margin as the author had not considered miscellaneous masses from wires, screws, and bolts.

Frame component	**Mass (g)**	**Description**
Bottom plate	91.354	Quadrotor arms are placed on this plate and battery is fitted between the top and bottom plates
Top plate	64.53	A plate to mount power distribution board and other electronic components
Flight controller platform	29.767	A plate above the top plate to mount the flight controller
Arms	296.1	Total mass of four arms in the quadcopter
Landing gear	149.474	Left and right legs of the landing gear
Camera holder	17.772	Camera mount for pitch movement and servo mount
Telemetry box	6.936	A holder for SiK radio telemetry box and antenna
Camera's antenna box	3.729	A holder for camera's 5.8GHz antenna
Total	659.663	Simulated total mass of the entire airframe

Table 5: Simulated masses of individual components making up the airframe assembly.

4.2.2 Static Stress Analysis

Static stress simulation was performed on the modelled airframe with PLA being the study material. Load was applied on each arm of the quadcopter where the motor and propeller would be placed to replicate the forces produced by propellers. The peak thrust produced by a 9450 propeller was 0.9kgf which was nearly 10N of force; thus, 10N was applied on each arm, along with gravitational force stressed on the whole frame. Fig. 11 represents the safety factor of

the design which indicates a maximum value of 15. This means that the airframe was over-engineered for 10N of force which was the reason 40% infill was initially planned to be used. Furthermore, the simulated stress level in Fig. 12a) was negligible with only 1.86MPa. Displacement and contact forces are shown in Fig. 12b). The displacement was the most concerning result as this could cause vibration and instability to the structure. The quadcopter's arm design had gone through several revisions to minimize the displacement below 0.5mm (Fig. 12b) in order to ensure safety and prevent high-frequency vibration from the rotation of motor and propeller. The contact forces occurred at the joints of components, yet these forces were insignificant, around 0.45MPa.

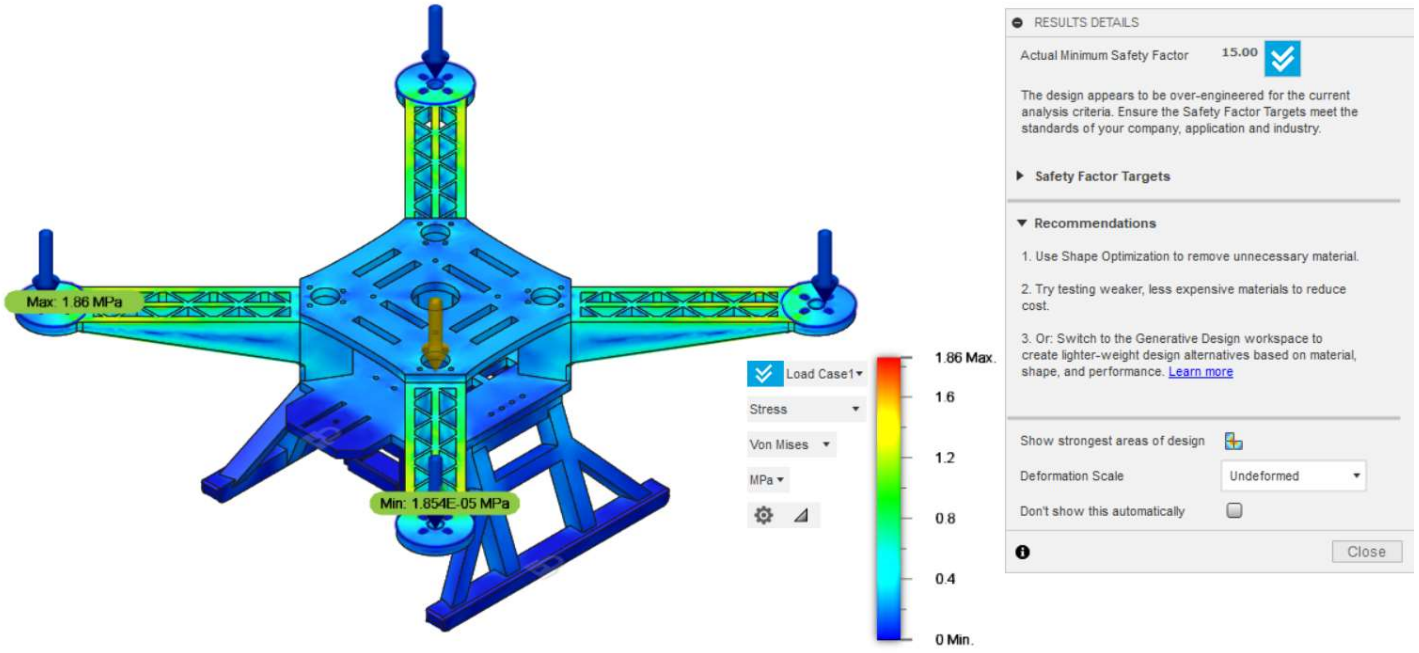

Figure 11: Static stress simulated result - safety factor and stress when 10N load was applied on each quadrotor arm.

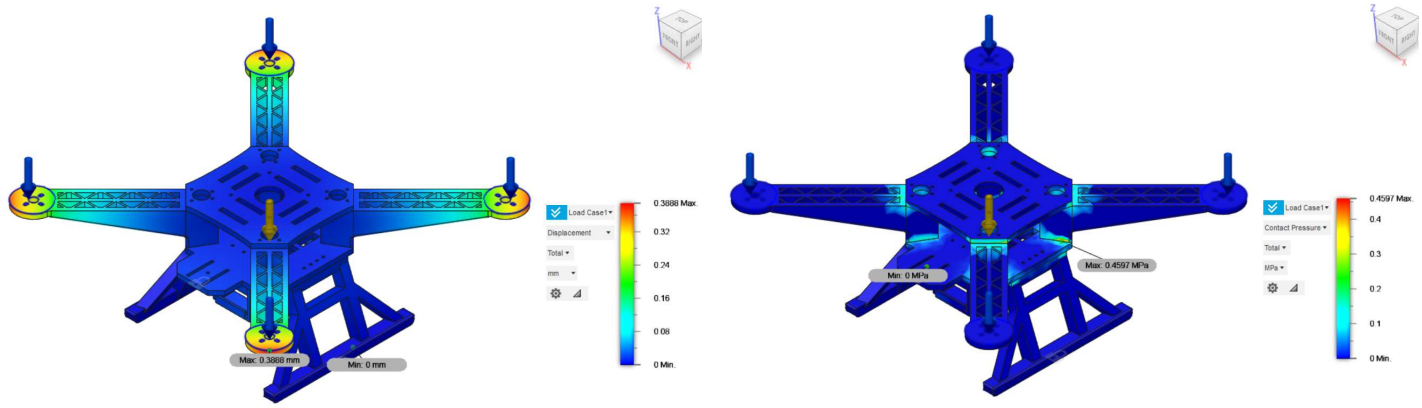

(a) Displacement (b) Contact pressure

Figure 12: Static stress simulated result – 10N force per quadrotor arm.

Apart from forces to simulate thrust produced by propellers, the moment was also considered. Fig. 13 and Fig. 14 show results when 120N.mm torque was generated on each arm of the quadcopter, combined with gravitational force. From

the figures, it is apparent that the design had high structural endurance to withstand peak torque generated by the 9450 propeller and 2312A/800Kv motor. The stress, displacement, and contact forces induced to the airframe due to peak torque of 120N.mm were negligible.

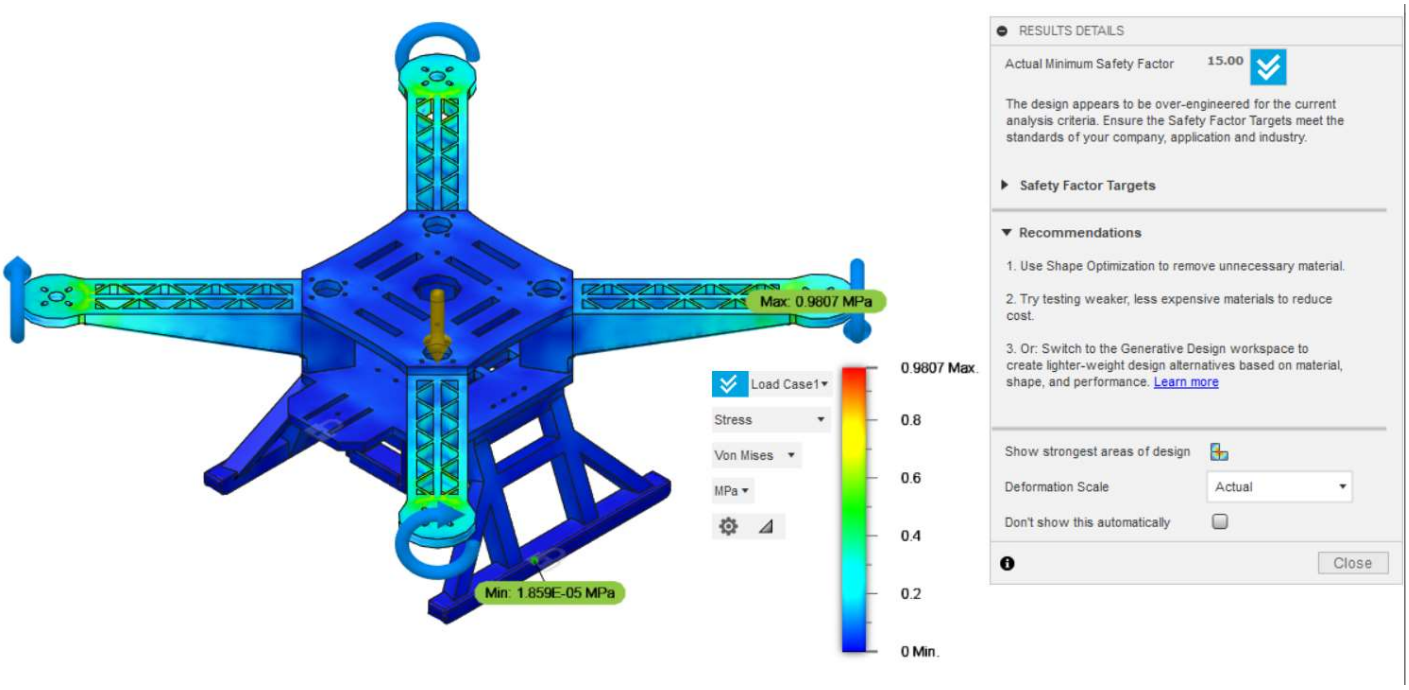

Figure 13: Static stress simulated result - safety factor and stress when 120N.mm torque was applied on each quadrotor arm.

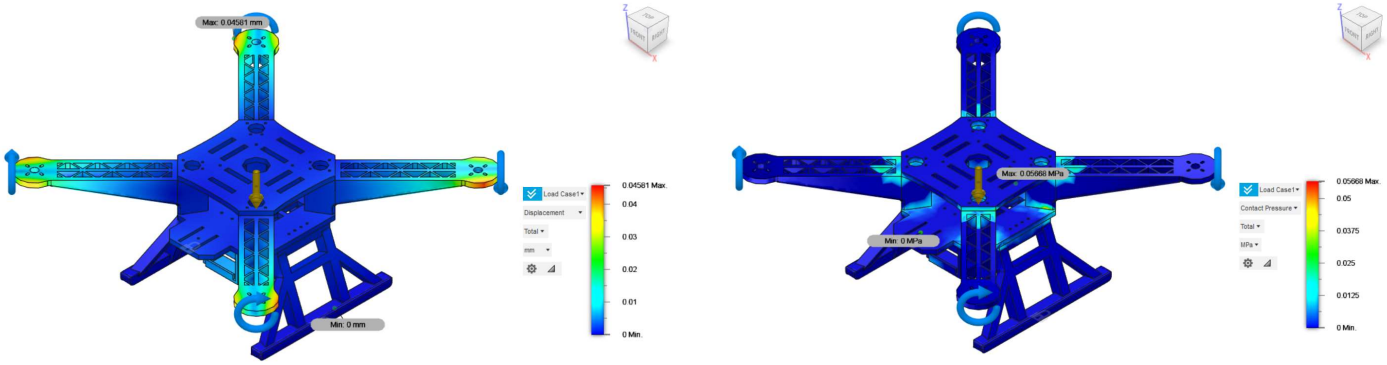

(a) Displacement (b) Contact pressure

Figure 14: Static stress simulated result – 120N.mm torque per quadrotor arm.

6. Implementation

After having finished the propulsion system design and 3D modelling for the quadcopter, the RPAS was constructed and assembled on a practical scale. Firstly, all necessary electronics components were installed on the completed airframe. Then, the flight controller was loaded with available autopilot firmware. Fig. 15 was used as a reference to connect all electronic components.

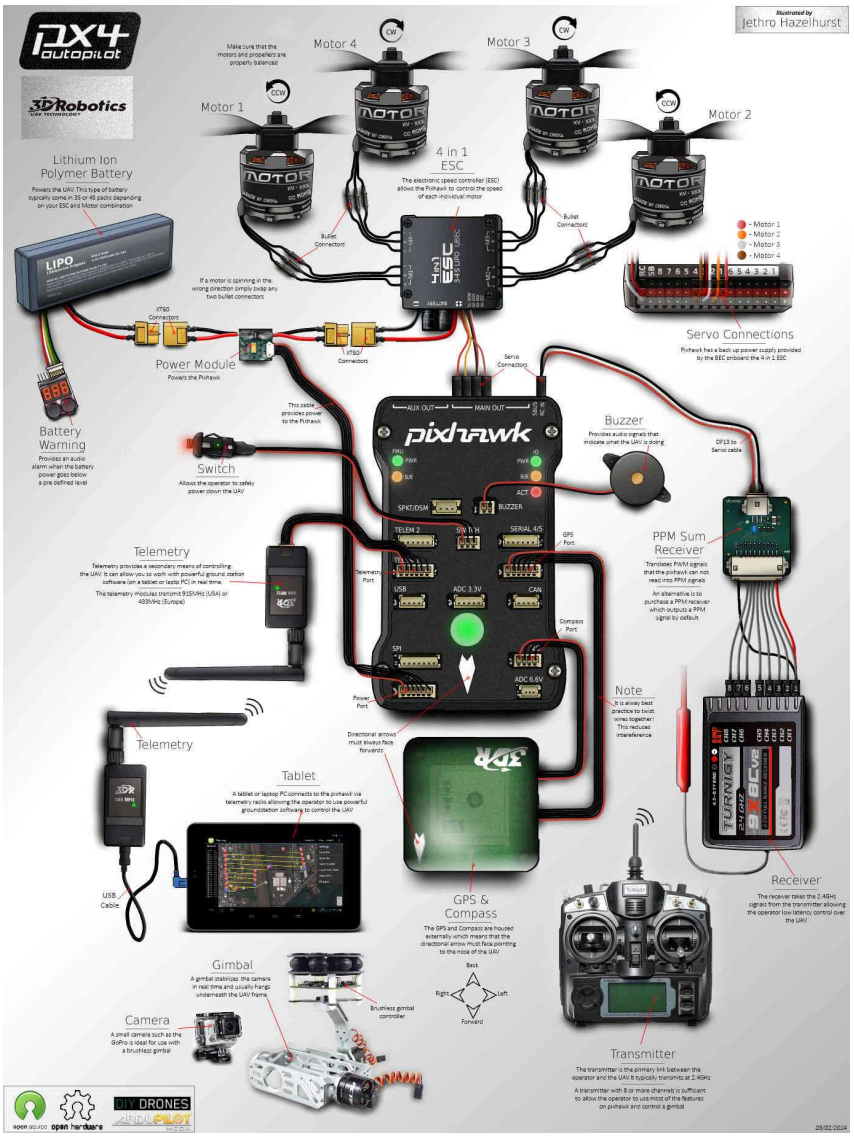

Figure 15: Pixhawk wiring chart for a quadcopter [18].

6.1 Hardware

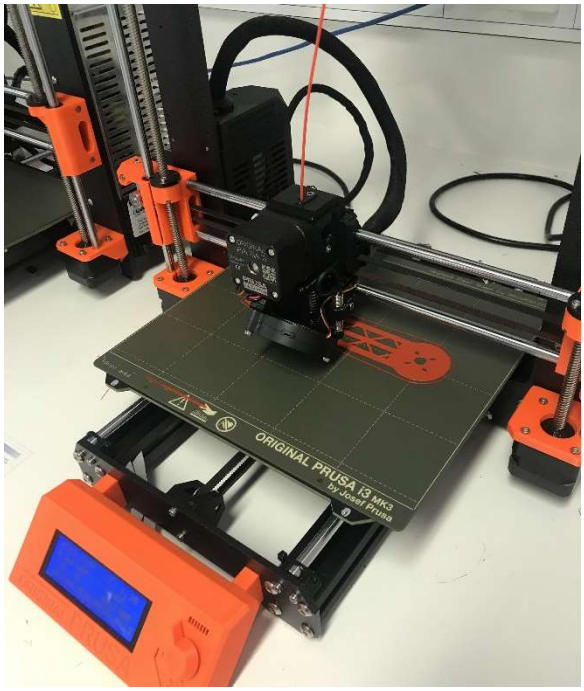

(a) 3D printing

(b) Weight of a quadrotor arm

Figure 16: Manufacturing process and weight measurement.

Each component making up the airframe assembly was 3D printed individually (Fig. 16a). Notable settings on Prusa Slicer, which is a software to export print files to Prusa i3 MK3 printers, were 40% infill percentage and gyroid infill type. Fig. 16b) shows the mass of a 3D printed quadcopter arm which was 48.72g. This mass was higher than simulated mass, 29.61g estimated from the Autodesk Fusion 360 software when 40% infill was applied. The same problem was seen in the entire airframe in which the actual airframe was heavier than the simulated results. The actual airframe weighed around 425g while the simulated results indicated a mass of 264g. Because of this, the completed RPAS with all required components were weighted which yielded the results in Table 6. At this point, the weights of motors, propellers, and ESCs were measured, indicating higher masses than estimation in section 1. The estimation at the beginning of this report was also missing power distribution board, screws, bolts, and standoffs. With the new weight measured from the completed RPAS, the propulsion system was re-evaluated to confirm its sufficiency in maintaining more than 2:1 thrust-to-weight ratio. The new thrust-to-weight ratio was now 2.46:1 instead of the desired 3:1 ratio. Assuming the total mass of the whole RPAS exceeds 1.8kg, which violates the 2:1 ratio, the 1045 propeller and 2810/1180Kv motor can be an alternative although this combination will reduce the endurance of the RPAS and will be a burden to the available budget.

Component	**Mass (g)**	**Description**
Airframe	427.93	40% infill, gyroid
Electronic components	244.68	Excluding battery, motors, propellers, and ESCs Including power distribution board
Motors	240	Total mass of 4 motors
Propellers	85	Total mass of 4 propellers
ESCs	44	Total mass of 4 ESCs
Battery	320	
Screws, bolts, standoffs, and wires	100	
Total	1461.61	

Table 6: Measured masses of components used in the final design.

Another problem occurred to the RPAS was in the landing gear. The first version of the landing gear showed to be very flexible to a point where it could break easily due to the brittleness characteristics of the material. This had also shown that the gear was generating vibration to the entire frame when the propeller was accelerating. Several revisions later had attempted to reduce the flexibility of the landing gear by applying ribs and more mechanical structure to the gear. These revisions can be seen in Fig. The landing gear was not properly designed due to the lack of simulation on the landing gear. The drop test, or event simulation, on Autodesk Fusion 360 was overseen while the static stress analysis could not underline the problem. Apart from the landing gear, the structure of the 3D-printed RPAS was rigid and stable. Fig. 18 shows two versions of the full-scale RPAS. Close-up images of some relevant components can be seen in Fig. 17

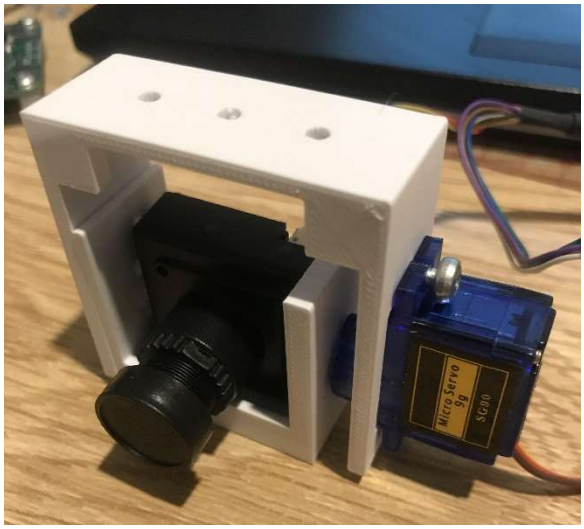

(a) Camera pitch mechanism

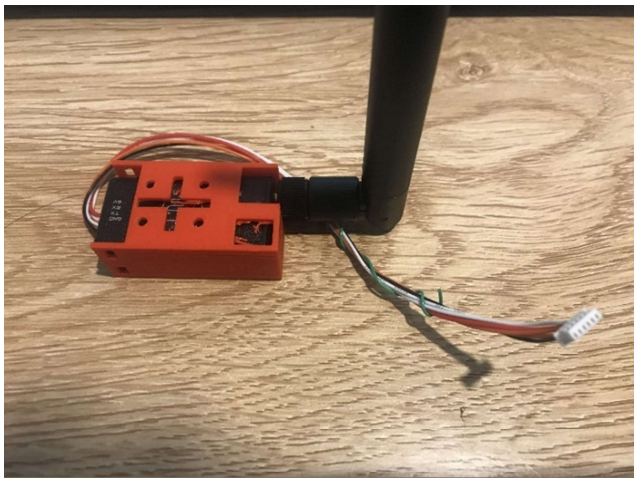

(b) Telemetry holder

© Rear undercarriage view

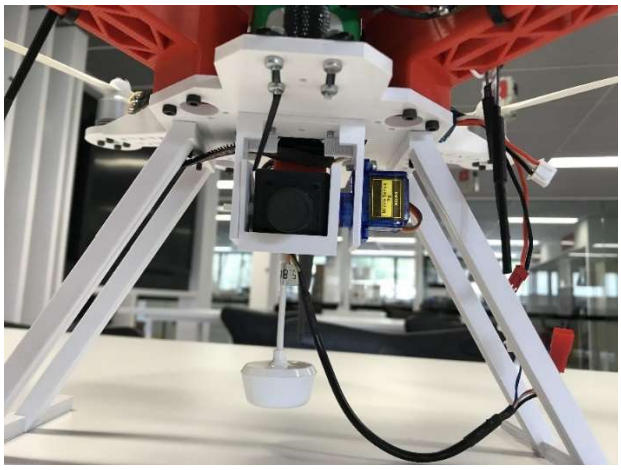

(d) Front undercarriage view

Figure 17: Full-scale final design hardware.

(a) Second revision

(b) Final design

Figure 18: Revisions of the RPAS.
The difference was in the landing gear and propellers.

6.2 Software

After the hardware of the RPAS had been set up, software configuration was carried out to install appropriate autopilot firmware onto the Pixhawk flight controller. Mission Planner was the ground control station (GCS) and was also the platform for all the software configurations. Some of the major configurations included:

- Frame type
- Accelerometer calibration
- Compass calibration
- Radio calibration
- Servo output settings
- ESC calibration
- Flight mode settings
- Failsafe configuration
- Motor test

Some of the mandatory settings for the Pixhawk are shown in Fig. 19

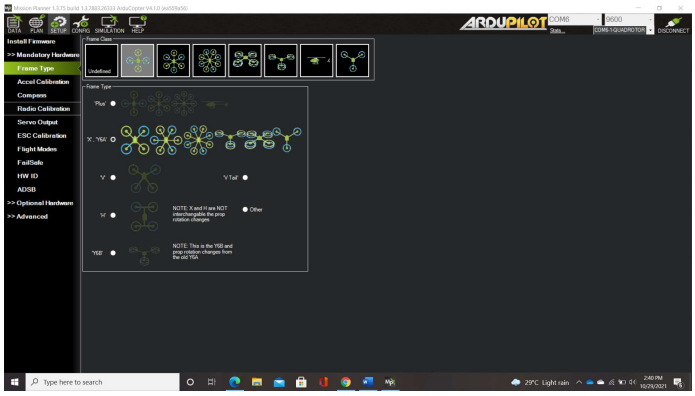

(a) Frame type

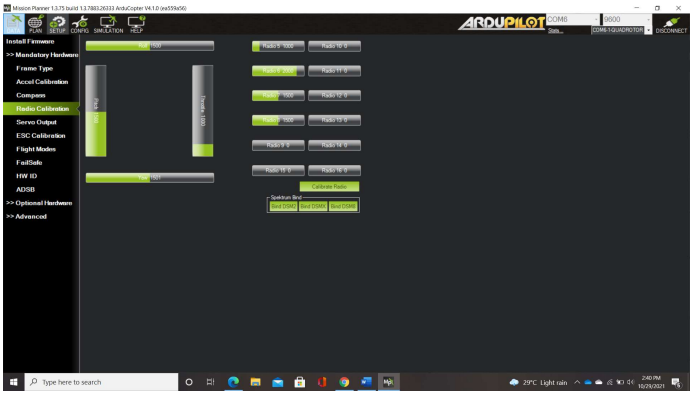

(b) Radio calibration

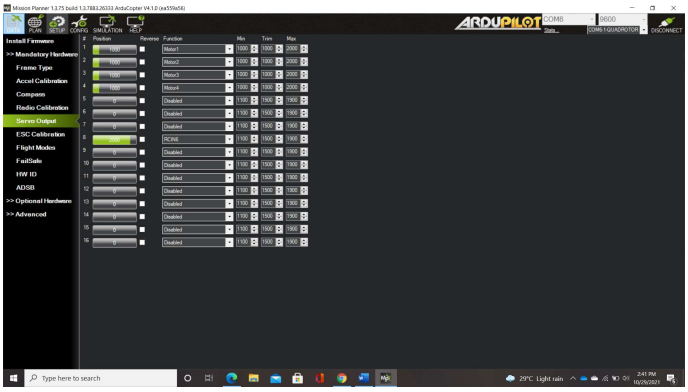

(c) Servo output settings

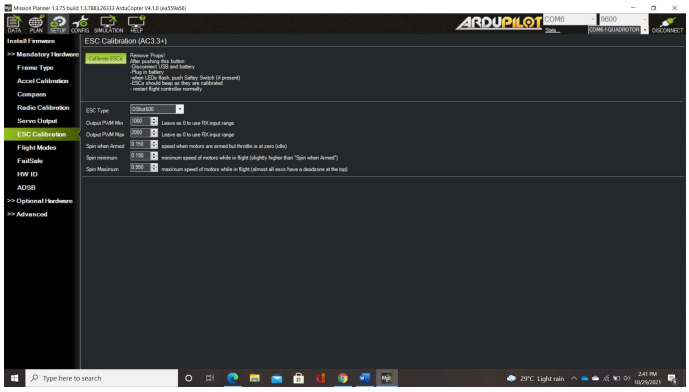

(d) ESC calibration

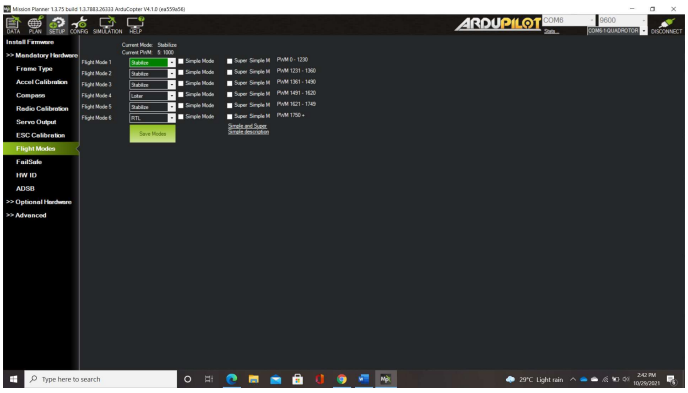

(d) Flight modes

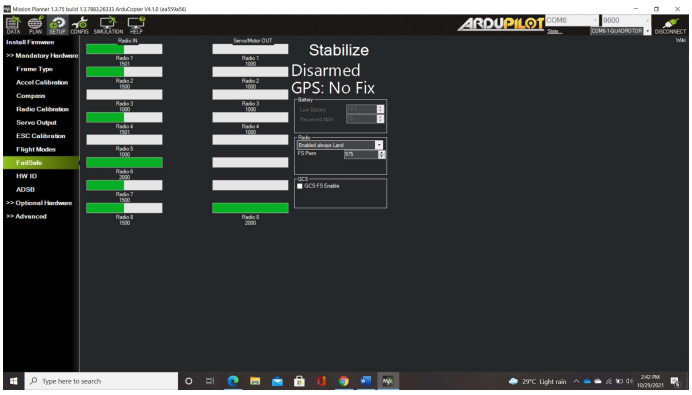

(e) Failsafe settings

Figure 19: Mission Planner configurations for Pixhawk 2.4.8.

7. Results

Initially, in some first flight tests, the quadcopter demonstrated abnormal behaviors during take-off in which one of the 9450 propellers spun faster than others resulted in the loss of balance for the entire RPAS. The RPAS had several crashes due to imbalance during take-off leading to the second version of the landing gear breaking. In addition, the second version of the landing gear vibrated when the propellers were accelerating, indicating that this version of the gear was not having sufficient strength to support the entire airframe. The new landing gear was designed and produced to improve the strength needed for harsh landing since all the flight tests were performed in stabilize mode without GPS. All three versions of the landing gear are shown in Fig. 20. Aggressive control was seen in stabilize mode where a slight input in the radio controller transmitter could lead to rapid movement of the RPAS. The RPAS seemed to have a difficult time during take-off which must be improved in the near future. The explanation for unstable take-off has not been identified at the time of this report. Decisive and quick throttle input was needed to make the quadcopter off the ground, yet it sometimes resulted in the quadcopter being tilted to one side where one of the propellers was not accelerating fast enough. The 9450 propellers had been replaced by 9443 propellers as one of the 9450 propellers was damaged slightly in one of the crashes. The black 9443 propellers mounted on the final design are shown in Fig 18b.

The camera mounted under the RPAS was working perfectly as it could pitch up and down using a potentiometer control on the RC transmitter. However, flight tests were done without the camera for safety reasons. Images of the RPAS in one of the flight tests are shown in Fig. 21.

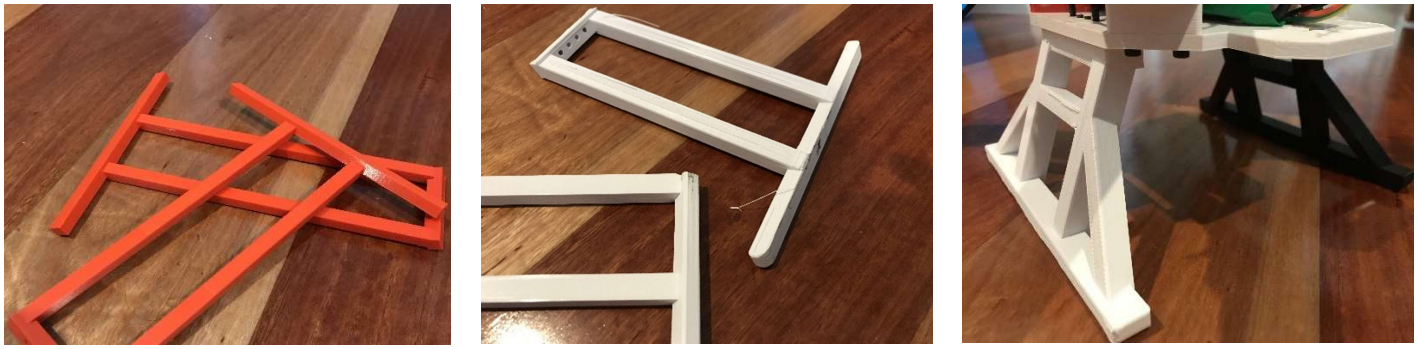

(a) First version (b) Second version - broken (b) Final design

Figure 20: All three versions of the landing gear for the RPAS.

(a) Take-off (b) Hover

Figure 21: Test flight in stabilize mode.

8. Conclusions and Future Work

After several test flights in stabilize mode, the RPAS seemed to behave well most of the time, indicating that the airframe and electronic components were designed and assembled properly. More flight tests are needed to investigate the problem behind the RPAS's imbalance in take-off which could be attributed to either PID tuning in the Mission Planner software or electronic hardware such as ESCs and motors. The operation of the RPAS had not been tested in GPS mode and with a camera payload. Therefore, flight tests relating to these features must be carried out in near future, but approval must be obtained from a certified CASA representative.

The landing gear was the weakest part of the airframe. The main reason this part was not properly designed was due to the lack of drop test, or event simulation, on 3D model software. The static stress analysis was significant in the airframe design phases as it gave an insight into how each component in the assembly behaved under large pressure. The airframe seemed to be overengineered as indicated by the simulated results. Therefore, future work can be done in an attempt to reduce the overall weight of the airframe.

References

[1] https://ieeexplore.ieee.org/stamp/stamp.jsp?tp=&arnumber=6196930

[2] https://epublications.marquette.edu/cgi/viewcontent.cgi?article=1370&context=theses_open

[3] http://philsal.co.uk/projects/uav/hadesmicro-quadcopter-flight-control-system

[4] https://www.tytorobotics.com/blogs/articles/how-to-increase-drone-flight-time-and-lift-capacity

[5] https://ardupilot.org/copter/docs/connect-escs-and-motors.html

[6] https://www.tytorobotics.com/blogs/articles/how-to-increase-drone-flight-time-and-lift-capacity

[7] https://www.tytorobotics.com/blogs/articles/the-drone-design-loop-for-brushless-motors-and-propellers

[8] https://github.com/MinhManLy/UAV-Design/blob/main/GU%206702ENG%20UAV%20Design/Lab%201%20Motor%20and%20Propeller%20Analysis/5inch%20and%206inch%20props/6702ENG%20Lab%20Report%20Props%20Motor%20Performance%20Analysis.pdf

[9] https://hobbyking.com/en_us/multistar-high-capacity-4s-4000mah-multi-rotor-lipo-pack.html?___store=en_us

[10] https://www.ovonicshop.com/products/ovonic-1300mah-4s-14-8v-100c-lipo-battery-with-xt60-for-fpv?variant=39280865280069&currency=AUD&utm_medium=product_sync&utm_source=google&utm_content=sag_organic&utm_campaign=sag_organic&gclid=Cj0KCQjwlOmLBhCHARIsAGiJg7ntY13u7gLr_8jtJiTGWKLunjj7htud-d2TDjp6onBgsu0dRbNQgLcaAtFVEALw_wcB

[11] https://www.ovonicshop.com/products/ovonic-1800mah-4s-14-8v-100c-lipo-battery-pack-with-xt60-plug?variant=39293785735237&currency=AUD&utm_medium=product_sync&utm_source=google&utm_content=sag_organic&utm_campaign=sag_organic&gclid=Cj0KCQjwlOmLBhCHARIsAGiJg7kUcYiGiNnlX9nazSS9b-ZyI-g6sAWOKiEhe7bTwiU7v37vgQywkQ8aAuq6EALw_wcB

[12] https://hobbyking.com/en_us/turnigy-high-capacity-battery-8000mah-4s-12c-drone-lipo-pack-xt90.html?wrh_pdp=6&utm_source=google&utm_medium=cpc&utm_campaign=google_au_shopping&countrycode=AU&gclid=Cj0KCQjwlOmLBhCHARIsAGiJg7m2Md54oW7-3qWtEtsQlOpZS3T7Jn8CHI60Cyrm73JdZsMdZTlLaE8aAoH7EALw_wcB

[13] https://www.ovonicshop.com/products/ovonic-14-8v-4s-5000mah-50c-hardcase-lipo-battery-pack-14-with-deans-plug?variant=39293642145861&currency=AUD&utm_medium=product_sync&utm_source=google&utm_content=sag_organic&utm_campaign=sag_organic&gclid=Cj0KCQjwlOmLBhCHARIsAGiJg7n0LscjAN-EekDlAgwMKBUYnnFQi-RPtifMeteu3_AOHtydyhHKBJcaAjQsEALw_wcB

[14] https://www.auselectronicsdirect.com.au/14.8v-5400mah-lipo-4s-battery-pack-with-deans-conn?gclid=Cj0KCQjwlOmLBhCHARIsAGiJg7lY82JY41x0eI6B0b_7cPIrIE-4e7k7YS_qCyYKSSQ_wSQY0L0XaIIaAjRXEALw_wcB

[15] https://www.pdfdrive.com/introduction-to-multicopter-design-and-control-e181096574.html [16] https://www.simplify3d.com/support/materials-guide/properties-table/

[17] https://dspace.mit.edu/bitstream/handle/1721.1/112940/Anderson_Physical%20and%20mechanical%20properties.pdf?sequence=1&isAllowed=y

[18] https://ardupilot.org/copter/docs/advanced-pixhawk-quadcopter-wiring-chart.html

Appendix A: Link to Resources

The documentation and relevant data of motor and propeller test can be found in the following repository:

https://github.com/MinhManLy/UAV-Design

The above link also serves as a logbook and will be updated if future work is to be carried out.

Appendix B: Mechanical Drawings

The mechanical drawing below is only for the bottom plate, top plate and four arms